Journal of Innate Immunity

Research Article

J Innate Immun 2023;15:351–364
DOI: 10.1159/000527649

Received: March 10, 2022
Accepted: October 17, 2022
Published online: November 30, 2022

The Olfactomedin-4-Defined Human Neutrophil Subsets Differ in Proteomic Profile in Healthy Individuals and Patients with Septic Shock

Hans Lundquist[a] Henrik Andersson[b] Michelle S. Chew[b] Jyotirmoy Das[c, d] Maria V. Turkina[e] Amanda Welin[a]

[a]Division of Inflammation and Infection, Department of Biomedical and Clinical Sciences, Faculty of Medicine and Health Sciences, Linköping University, Linköping, Sweden; [b]Department of Anaesthesia and Intensive Care, Biomedical and Clinical Sciences, Faculty of Medicine and Health Sciences, Linköping University, Linköping, Sweden; [c]Bioinformatics, Core Facility, Division of Cell Biology, Department of Biomedical and Clinical Sciences, Faculty of Medicine and Health Sciences, Linköping University, Linköping, Sweden; [d]Clinical Genomics Linköping, SciLife Laboratory, Department of Biomedical and Clinical Sciences, Faculty of Medicine and Health Sciences, Linköping University, Linköping, Sweden; [e]Department of Biomedical and Clinical Sciences, Faculty of Medicine and Health Sciences, Linköping University, Linköping, Sweden

Keywords
Olfactomedin-4 · Neutrophil subpopulations · Proteome · Sepsis

Abstract
The specific granule glycoprotein olfactomedin-4 (Olfm4) marks a subset (1–70%) of human neutrophils and the Olfm4-high (Olfm4-H) proportion has been found to correlate with septic shock severity. The aim of this study was to decipher proteomic differences between the subsets in healthy individuals, hypothesizing that Olfm4-H neutrophils have a proteomic profile distinct from that of Olfm4 low (Olfm4-L) neutrophils. We then extended the investigation to septic shock. A novel protocol for the preparation of fixed, antibody-stained, and sorted neutrophils for LC-MS/MS was developed. In healthy individuals, 39 proteins showed increased abundance in Olfm4-H, including the small GTPases Rab3d and Rab11a. In Olfm4-L, 52 proteins including neutrophil defensin alpha 4, CXCR1, Rab3a, and S100-A7 were more abundant. The data suggest differences in important neutrophil proteins that might impact immunological processes. However, in vitro experiments revealed no apparent difference in the ability to control bacteria nor produce oxygen radicals. In subsets isolated from patients with septic shock, 24 proteins including cytochrome b-245 chaperone 1 had significantly higher abundance in Olfm4-H and 30 in Olfm4-L, including Fc receptor proteins. There was no correlation between Olfm4-H proportion and septic shock severity, but plasma Olfm4 concentration was elevated in septic shock. Thus, the Olfm4-H and Olfm4-L neutrophils have different proteomic profiles, but there was no evident functional significance of the differences in septic shock.

Introduction

The neutrophil granulocyte, the most abundant of the leukocytes, is today recognized as a heterogenous cell type with distinct subsets [1]. The glycoprotein olfactomedin-4 (Olfm4) marks such a subset in humans as well as in mice [2–5]. Olfm4 is a constitutive human neutrophil subset marker, meaning that the Olfm4 protein is present in only a subset of neutro-

Karger@karger.com
www.karger.com/jin

Correspondence to:
Amanda Welin, amanda.welin@liu.se

phils in the peripheral blood of a given individual [2, 3, 5], independently of cell activation status or age [3].

The Olfm4 protein locates to the specific granules of neutrophils [2, 3]. As determined by fluorescence in situ hybridization, all granulocyte precursors express Olfm4 mRNA at the myelocyte and metamyelocyte stages, indicating that an unknown post-transcriptional mechanism determines whether the protein is translated [2]. The proportion of Olfm4-high (Olfm4-H) neutrophils varies between individuals (1–70% of neutrophils) [2–4, 6] and healthy blood donors display low variation in the proportion of Olfm4-H neutrophils over time [3]. Meanwhile, proportional fluctuations over time have been observed in children after bone marrow transplantation [7], and an increase in the Olfm4-H proportion has been observed following haemorrhagic shock [8]. The function of human Olfm4 and potential differential functions of the subset are not known.

We have previously shown that the Olfm4-defined neutrophil subsets have equal tendency to phagocytose bacteria, undergo apoptosis, and transmigrate to inflamed tissue and that Olfm4 can be found in a subset of neutrophil extracellular traps [3]. It has more recently been discovered that the proportion of Olfm4-H neutrophils correlates with the severity of paediatric septic shock [4] and can independently predict mortality in adult septic shock [6]. Earlier mouse studies suggested a detrimental effect of Olfm4 during bacterial infection, with mice lacking Olfm4 having an enhanced capacity to combat *Staphylococcus aureus* and *Escherichia coli* as well as prevent colonization with *Helicobacter pylori* [9].

Sepsis is a leading cause of death among hospitalized patients worldwide with a mortality rate of ~20% [10]. According to the consensus definition Sepsis-3 [11], sepsis is life-threatening organ dysfunction caused by a dysregulated host response to infection. Septic shock is a subset of sepsis in which the underlying circulatory and cellular metabolism abnormalities are profound enough to substantially increase mortality. The septic immune response is multifaceted with components of exaggerated activation and immune suppression, and the response varies between individuals [12]. During the septic immune response, the innate immune system is severely dysregulated. Neutrophil granulocytes contribute to microbe clearance but are also inappropriately activated leading to immunopathology [12, 13]. Consequently, the finding that the Olfm4-H neutrophil proportion correlates with the severity and outcome of sepsis [4, 6] warrants investigation into the differential contributions of the subsets to immune dysfunction in sepsis.

The primary aim of this study was to decipher proteomic differences between the Olfm4-defined human neutrophil subsets at baseline, with the hypothesis that Olfm4 marks a neutrophil subset with a distinct proteomic profile. Secondly, we aimed to investigate whether these proteomic differences exist also in septic shock, possibly contributing to sepsis pathogenesis.

Materials and Methods

Patient Characteristics and Data Collection

Adult patients (>18 years old) admitted to the intensive care unit (ICU) at Linköping University Hospital with a diagnosis of septic shock using the Sepsis-3 criteria were included within 12 h of admission. Acute coronary syndrome at presentation was an exclusion criterion. The patients were part of a larger on-going, prospective study (NCT04695119). The mean age of the 20 patients included for analysis of Olfm4-H proportion and plasma Olfm4 concentration was 67 years (range 46–85); 12 were males and 8 females. Data on sequential organ failure assessment (SOFA) score on admission and number of days alive and free of invasive ventilatory, renal, or haemodynamic support within 30 days, termed organ support-free days (OSFDs), were collected. The SOFA score is the predominant score quantifying the severity of organ dysfunctions in sepsis [11], and OSFD is a commonly used proxy of outcome in septic shock studies [14]. The outcome measures were the correlation between the percentage of Olfm4-H neutrophils and SOFA score or OSFD and between the plasma concentration of Olfm4 and SOFA score or OSFD.

Neutrophil Isolation

Prior to processing for proteomics, neutrophils were isolated by means of density gradient centrifugation from 18 mL of whole blood obtained from healthy blood donors through the Linköping University Hospital blood bank, or 3 mL from patients with septic shock (see above), within 3 h of blood collection into EDTA BD Vacutainer blood collection tubes (Becton Dickinson, Franklin Lakes, NJ, USA). The blood was then layered onto a gradient of Polymorphprep (Alere Technologies, Oslo, Norway) and Lymphoprep (Alere Technologies) according to the manufacturer's instructions. Briefly, tubes were centrifuged in a swing-out centrifuge for 40 min, 480 *g* at room temperature (RT), and the granulocyte band washed in phosphate-buffered saline (PBS) at RT. Remaining erythrocytes were lysed with distilled H_2O at 4°C and the granulocytes washed twice with Krebs-Ringer glucose (KRG) phosphate buffer at 4°C, resuspended in PBS on ice, and processed immediately.

Antibody Staining and FACS

For sorting into neutrophil subsets, isolated granulocytes were stained for surface CD15 followed by intracellular Olfm4. First, 2×10^7 cells resuspended in 0.5 mL PBS were incubated with PE-conjugated mouse anti-human CD15 antibody (BioLegend, San Diego, CA, USA) at 2.5 μg/mL, for 30 min on ice. Cells were then washed in PBS and resuspended in 1 mL cold BD Cytofix/Cytoperm (Becton Dickinson) for fixation and permeabilization, incubating for 20 min on ice. After washing twice with cold BD

Perm/Wash (Becton Dickinson), the cells were resuspended in 1 mL BD Perm/Wash containing rabbit anti-Olfm4 serum (prepared in-house and kindly provided by Dr. Matthew Alder, Cincinnati Children's Hospital, OH, USA [7]), diluted 1:400, and incubated for 30 min at RT. The cells were washed twice and resuspended in 1 mL BD Perm/Wash containing AlexaFluor 647-conjugated goat anti-rabbit IgG (Thermo Fisher Scientific, Waltham, MA, USA) at 5 μg/mL, incubating for 30 min at RT. After three final washing steps, the pellet was resuspended in 300 μL PBS for fluorescence-activated cell sorting (FACS).

The stained granulocytes were sorted into two populations: CD15-high and Olfm4-H or CD15-high and Olfm4-low (Olfm4-L) neutrophils, on a BD FACSAria III Cell Sorter (Becton Dickinson). Between 1×10^6 and 5.5×10^6 cells per subset were sorted, depending on the subset proportions in different individuals. The gating strategy is shown in online supplementary Figure S1 (see www.karger.com/doi/10.1159/000527649 for all online suppl. material).

Peptide Preparation and LC-MS/MS

A protocol for the preparation of formaldehyde-fixed tissue for subsequent liquid chromatography with tandem mass spectrometry (LC-MS/MS) analysis published by Coscia et al. [15] was adapted to formaldehyde-fixed neutrophils in suspension. Sorted neutrophils were pelleted and resuspended in 100 μL lysis buffer (300 mM Tris/HCl in 50% acetonitrile, pH 8). Samples were sonicated using a Fisherbrand model 705 Sonic Dismembrator (Thermo Fisher Scientific) for 2 cycles (5 s on/off) at 40 amplitude and placed in a heating block for 90 min at 90°C. To reduce proteins, samples were incubated in 5 mM 1,4-dithiothreitol (Roche, Basel, Switzerland) for 20 min, mixing at 1,400 RPM, at RT. Then, to alkylate proteins, 25 mM iodoacetamide (Merck, Darmstadt, Germany) was added and samples incubated for a further 30 min, mixing at 1,400 RPM, at RT in the dark. Protein samples were vacuum concentrated to about 20 μL using a CHRIST RVC 2–25 centrifuge (Martin Christ Gefriertrocknungsanlagen, Osterode am Harz, Germany) set to 60°C. The protein concentration was measured by NanoDrop (Thermo Fisher Scientific) at 280 nm, and 100 μg of protein was digested by adding MS grade Pierce Trypsin Protease (Thermo Fisher Scientific) at a protein/trypsin ratio of 1:50 and 10% acetonitrile (Thermo Fisher Scientific), in a final volume of 100 μL. Samples were incubated overnight, shaking at 1,400 RPM, at 37°C.

Peptide samples were acidified by adding 1% trifluoroacetic acid (Merck) and debris pelleted by centrifugation for 5 min at 14,000 *g*. Peptide clean-up was performed using Pierce C18 tips (Thermo Fisher Scientific) following the manufacturer's instructions, eluting using 80% acetonitrile (Thermo Fisher Scientific). Eluted samples were dried completely by CHRIST RVC 2–25 centrifuge at 45°C and resuspended in 15 μL 0.1% formic acid (Sigma-Aldrich, Saint Louis, MO, USA), vortexed and sonicated in an ultrasonic water bath for 10 min. After a further concentration measurement, samples were diluted to 0.1 μg/μL in 0.1% formic acid in MS autosampler vials (Thermo Fisher Scientific). Five microlitres of peptides were loaded onto an Easy nanoLC (Thermo Fisher Scientific) coupled to a Q Exactive HF Hybrid Quadrupole-Orbitrap Mass Spectrometer (Thermo Fisher Scientific). Peptides were separated by reverse phase chromatography using a C18 pre-column (Acclaim PepMap 100, 75 μm × 2 cm, Thermo Fisher Scientific) followed by C18 reversed-phase LC column (PepMap RSLC C18, 2 μm, 100A 75 μm × 25 cm, Thermo Fisher Scientific) on EASY nLC 1200 system (Thermo Fisher Scientific). A linear gradient from 0.1% formic acid in H_2O (A) to 0.1% formic acid in 80% acetonitrile (B) was applied at a flow rate of 300 nL/min as follows: from 6% B to 28% B at 50 min; from 28% B to 40% B at 78 min, 100% B at 95 min. Measurements were taken in positive polarity, Full MS to dd-MS^2 mode. Resolution was 120,000 with a range of 380–1,400 m/z and an automatic gain control target of 3×10^6 and 120 ms ion time.

Bioinformatics

Obtained RAW files were analysed in Proteome Discoverer 2.5.0.4 (Thermo Fisher Scientific) using a human reference proteome database (79,038 entries, downloaded from Uniprot February 15, 2022). MSPepSearch and Sequest HT were searched in sequence, keeping medium confidence peptides between, with fragment mass tolerance set to 0.15 Da and precursor mass tolerance set to 14 PPM. Full trypsin digestion and a maximum of two missed cleavages as well as a minimum peptide length of 6 amino acids was specified. Carbamidomethyl of cysteine was specified as a fixed modification and oxidation as dynamic modification. Percolator validation used standard settings. Label-free quantification was carried out to calculate abundances of proteins in Olfm4-H and Olfm4-L neutrophil samples. Unique and razor peptides were considered in protein quantification. Precursor abundance was based on intensity. To account for experimental bias, normalization of protein abundances was based on a set of proteins previously described as neutrophil "housekeeping proteins" [16] and imputation was set to replicate-based resampling. Peptides of less than medium confidence were filtered out and proteins were identified by at least 2 peptides. Protein abundances were calculated by summing sample abundances of connected peptide groups. Median-paired Olfm4-H/L log2 ratio calculations were based on all possible pairwise ratios of connected peptides between replicates and tested for significant difference by a background-based *t* test with Benjamini-Hochberg correction. Proteome Discoverer filters were set to include high-confidence master proteins with an abundance value in both Olfm4-H and Olfm4-L groups. Proteins in the Olfm4-H and Olfm4-L samples where the log2 abundance ratio had a p value of <0.05 were considered and the corresponding gene symbols used as input for pathway enrichment analysis in the Reactome pathway database (https://reactome.org/; release 79) [17] with regard to the human genome. Reactome is free, open-source, open-data, and peer-reviewed knowledgebase of biomolecular pathways providing high-quality curated data over other open-source databases [18]. A minimum of 5 genes were considered to calculate significantly enriched pathways with Benjamini-Hochberg-corrected p value <0.05.

Immunofluorescent Validation of Protein Abundance

Granulocytes were isolated from 1-day-old buffy coats from healthy blood donors, diluted 1:5 in 0.85% NaCl at RT, by routine methods as described above. Two million cells were fixed using BD Cytofix/Cytoperm and intracellularly stained for Olfm4 with the addition of 60 nM DAPI in the secondary antibody step. Anti-Olfm4 serum as described above or commercial rabbit anti-human Olfm4 (HPA077718, Atlas antibodies, Stockholm, Sweden) at 2 μg/mL were used. The commercial antibody was first validated against the anti-Olfm4 serum (online suppl. Fig. S2). To quantify proteins of interest as identified by proteomics, AlexaFluor

488-conjugated mouse anti-human Rab3d (sc-398727, Santa Cruz Biotechnology, Dallas, TX, USA) at 10 μg/mL, AlexaFluor 488-conjugated mouse anti-human S100A7 (NBP2-24911AF488, Novus Biologicals, Abingdon UK) at 31.5 μg/mL, AlexaFluor 488-conjugated mouse anti-human Rab3a (sc-365069, Santa Cruz Biotechnology) at 10 μg/mL or fluorescein isothiocyanate-conjugated mouse anti-human CXCR1 (320605, BioLegend) at 5 μg/mL were included in the primary antibody step. Cells were finally resuspended in 20 μL PBS and analysed by imaging flow cytometry using an ImageStream MK II (Luminex corporation, Austin, TX, USA). At least 20,000 events were acquired at ×60 magnification. IDEAS version 6.2 was used for analysis. After applying a colour compensation matrix, neutrophils and Olfm4-H and Olfm4-L populations were gated as described in online supplementary Figure S3. Specific staining was verified using a matching isotype control for each antibody. Median overall fluorescence intensity of the proteins of interest in Olfm4-H and Olfm4-L neutrophils, respectively, is reported.

Analysis of ROS Production in Neutrophil Subsets

Granulocytes were isolated as described above from buffy coats obtained from healthy blood donors and 8×10^7 cells were resuspended in 50 μL KRG supplemented with 1 mM Ca^{2+} and placed in a 37°C heat block. The fixable DNA-binding radical oxygen species (ROS) dye CellROX Green (Thermo Fisher Scientific) was added at 2.5 μM and the cells incubated for 15 min for dye uptake. The cells were stimulated with 25 μM phorbol 12-myristate 13-acetate (PMA; Merck, Darmstadt, Germany), or buffer as a negative control, for 5 min. Finally, the cells were washed, fixed, permeabilized, and stained for Olfm4 and DNA as described above, followed by imaging flow cytometry analysis. At least 10,000 events per sample were acquired, and data were analysed using the gating strategy described in online supplementary Figure S3. The median CellROX intensity in the Olfm4-H and Olfm4-L populations is reported.

Bacterial Infection Assay

Staphylococcus aureus strain RN4220 containing the pCN-GFP plasmid for green fluorescent protein (GFP) production was cultured in lysogeny broth supplemented with 10 μg/mL erythromycin for plasmid selection. Fifty microliter of overnight culture was diluted in 10 mL lysogeny broth and cultured to mid-log phase (optical density ≈0.5) and the bacterial concentration determined using a standard curve. Neutrophils were isolated from buffy coats obtained from healthy blood donors, as described above. Then, *S. aureus* at a multiplicity of infection of 10 was added to 2×10^7 neutrophils suspended in 1 mL cold KRG supplemented with 1 mM Ca^{2+}. Bacteria were allowed to adhere to the neutrophil surface by incubation on ice for 15 min. To remove unbound bacteria, samples were washed twice by centrifugation at 300 *g* for 5 min at 4°C, removal of the supernatant, and resuspension in cold KRG with Ca^{2+}. Where applicable, 10 μM of the NADPH-oxidase inhibitor diphenyleneiodonium chloride or 1% dimethyl sulfoxide (DMSO) as a solvent control was then added. The samples were placed in a 37°C heat block for the indicated times, upon which they were removed and placed on ice. After one wash in cold PBS, samples were fixed, permeabilized, and stained for Olfm4 and DNA as described above. At least 2,000 events were acquired on an imaging flow cytometer, and the number of bacteria per neutrophil was analysed using a custom-made spot counting feature in the analysis software IDEAS (online suppl. Fig. S3). The mean number of fluorescent bacteria per cell over time in Olfm4-H and Olfm4-L neutrophils is reported. The presence of GFP and viability of *S. aureus* do not correlate fully [19]; thus, the assay was used to determine ability to control rather than kill the bacteria.

Olfm4-H/L Proportions in Low Density and Normal Density Neutrophils

Neutrophils were isolated from buffy coats obtained from healthy blood donors, stained for CD15, fixed, permeabilized, and stained for Olfm4 as described above. In parallel, the peripheral blood mononuclear cell (PBMC) layer from the same blood donors were processed in the same way. 10,000 cells from the granulocyte layer and at least 60,000 cells from the PBMC layer were acquired on an imaging flow cytometer, and the proportion of Olfm4-H neutrophils was analysed in the respective samples, the cells from the granulocyte layer representing normal density neutrophils (NDN) and those from the PBMC layer low density neutrophils (LDNs). The gating strategy is described in online supplementary Figure S3.

Olfm4-H/L Proportions in Neutrophils Obtained from Patients with Septic Shock

Whole blood from patients with septic shock (3 mL) was collected and processed for Olfm4-H/L proportion analysis, without prior cell separation, within 3–20 h. Control experiments where blood from 3 healthy donors was processed immediately upon arrival or incubated for 20 h at RT before processing showed no impact of incubation on the percentage of Olfm4-H neutrophils (online suppl. Fig. S4). To fix leukocytes and remove erythrocytes, 400 μL of blood was treated with BD FACS lysing solution (Becton and Dickinson) according to the manufacturer's instructions. Plasma was separated from the remaining blood volume and frozen at −70°C for later use. The fixed leukocytes were stained for CD15 followed by permeabilization and staining of Olfm4 as described above, with the addition of DAPI. Each patient sample was stained in parallel with a sample from a healthy blood donor. The cells were resuspended in 20 μL PBS for imaging flow cytometry. The size of the Olfm4-H neutrophil subset was determined using imaging flow cytometry, where at least 1,500 events were acquired. Cells were gated as described in online supplementary Figure S3, identifying the Olfm4-H and Olfm4-L populations based on Olfm4 intensity. The gate for Olfm4-H was set based on a negative control for each donor, omitting the primary antibody.

Olfactomedin-4 and NGAL ELISA

After centrifugation of thawed plasma samples at 2,000 *g* for 10 min and dilution of samples by 1:10, 1:20, or 1:100, the Human Olfm4 SimpleStep ELISA kit (ab267805, Abcam, Cambridge, United Kingdom) and LEGEND MAX™ Human neutrophil gelatinase-associated lipocalin (NGAL) ELISA kit (cat#443407, BioLegend, San Diego, CA, USA) were performed in duplicate according to the manufacturers' instructions. The Olfm4 concentration was calculated using a linear standard curve while NGAL concentration was calculated using 5-parameter logistic curve fit. The mean concentration of the duplicates is reported. In addition, Olfm4 concentration was normalized to the neutrophil concentration in the original blood sample, as estimated from imaging flow cytometry sample information. Since some patient samples were processed the morning after blood collection (see above), we examined whether incubation of the blood affected the plasma Olfm4 concentration. Incubation of blood from healthy blood donors for

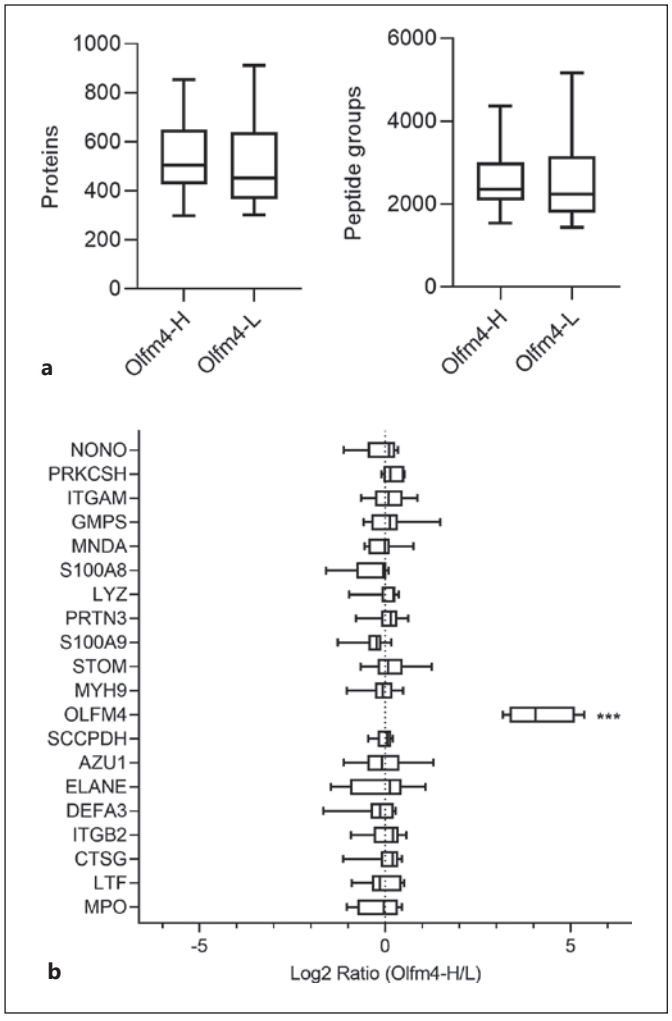

Fig. 1. Proteomic analysis of Olfm4-defined neutrophil subsets in healthy blood donors. Olfm4-H and Olfm4-L neutrophils isolated from healthy blood donors (n = 8) were stained, sorted by FACS, and analysed by LC-MS/MS. **a** Box-and-whisker plots showing the number of proteins and peptide groups identified in Olfm4-H and Olfm4-L neutrophil samples. **b** Box-and-whisker plot showing protein abundance log2 ratios for the 20 most abundant proteins between paired Olfm4-H/L neutrophil samples. Common contaminants and histones are not shown.

20 h did not significantly affect the concentration of Olfm4 in plasma, as compared to immediate processing (online suppl. Fig. S4).

Statistical Methods

Statistical analysis was performed using GraphPad Prism, v. 9.2.0 (see above for statistical analysis of proteomics data). All box-and-whisker plots depict median and interquartile range. Differences between groups were analysed as described in the figure legends and the result considered significant at $p < 0.05$. Throughout the manuscript, significant differences are denoted by *($p < 0.05$), **($p < 0.01$), or ***($p < 0.001$).

Results

The Olfm4-Defined Neutrophil Subsets from Healthy Donors Exhibit Different Proteomic Profiles

To test the hypothesis that Olfm4 marks a neutrophil subset with a distinct proteomic profile, the proteomes of FACS-sorted Olfm4-H and Olfm4-L resting neutrophils from healthy blood donors were analysed. A published method [15] was adapted to suit neutrophils in suspension, enabling analysis of formaldehyde-fixed, permeabilized, and antibody-stained neutrophils by LC-MS/MS. The approach yielded a similar number of proteins and peptide groups identified in both subsets (Fig. 1a). In total, 1,136 protein were identified in both Olfm4-H and Olfm4-L neutrophil samples. Online supplementary Table S1 lists all the identified proteins and their abundance in each subset. Among the 20 proteins with the highest abundance, major neutrophil granule proteins such as lysozyme, myeloblastin, S100A8/A9, azurocidin, neutrophil elastase, cathepsin G, lactoferrin, and myeloperoxidase were found, and none of these displayed significantly increased abundance in either subset. Olfm4 was detected among the 20 most abundant proteins in the Olfm4-H subset, and although there was a clear difference in abundance of Olfm4 between the subsets with a nearly 24-fold increase in the Olfm4-H subset, Olfm4 was detected in both populations (online suppl. Table S1). Thus, we use the terms "Olfm4-H" and "Olfm4-L" rather than "Olfm4 positive" and "Olfm4 negative." The relative abundance of each protein between the Olfm4-H and Olfm4-L subsets was analysed in terms of log2 abundance ratio, where a positive value means a higher median abundance in the Olfm4-H subset and vice versa. Olfm4 had a median log2 ratio between the Olfm4-H and Olfm4-L subsets of 4.1, with a significance level of $p = 8.0 \times 10^{-16}$ (Fig. 1b).

A log2 abundance ratio between the Olfm4-H and Olfm4-L subsets with a p value of <0.05 was observed for 91 proteins, where 39 proteins were more abundant in the Olfm4-H and 52 in the Olfm4-L subset (Fig. 2a). Several proteins relevant to the neutrophil immune response such as Rab3d, Rab11A, and leucine-rich alpha-2 glycoprotein showed higher abundance in the Olfm4-H subset (Fig. 2b, left panel). Meanwhile, neutrophil defensin alpha 4, C-X-C chemokine receptor type 1 (CXCR1), Rab3a, and S100-A7 among others displayed higher abundance in the Olfm4-L subset (Fig. 2b, right panel).

The list of differentially abundant proteins converted to gene symbols was used as the input list to the Reactome database for pathway enrichment analysis. In healthy

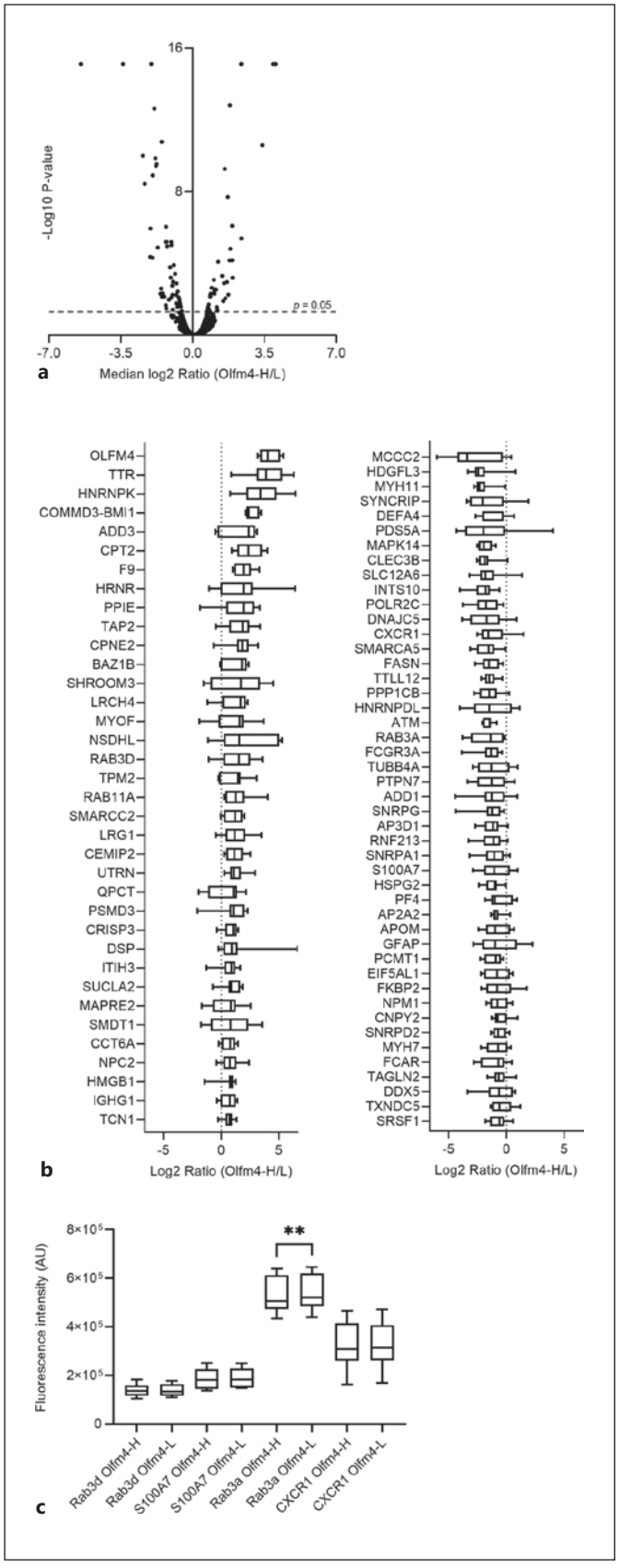

blood donors, the Olfm4-H subset showed significant enrichment in the pathways neutrophil degranulation ($p = 3.0 \times 10^{-7}$) and innate immune system ($p = 0.0018$) (online suppl. Table S2) and the Olfm4-L subset in the neutrophil degranulation pathway ($p = 0.043$), as well as several pathways related to mRNA splicing (online suppl. Table S2).

To validate the differential abundance of selected proteins with functions relevant to the neutrophil immune response, immunofluorescent staining and imaging flow cytometry analysis were used. Neutrophil Olfm4 was thus stained in combination with Rab3d (increased in Olfm4-H), Rab3a, S100-A7, or CXCR1 (increased in Olfm4-L). As shown in Figure 2c, the intensity of Rab3a was significantly higher ($p = 0.0078$) in the Olfm4-L subset. The other proteins were not significantly increased in either subset and none of the investigated proteins displayed a bimodal distribution.

Olfm4-H and Olfm4-L Neutrophils Have Equal Potential for ROS Production, Ability to Control S. aureus, and Tendency to Appear in the LDN Fraction

Having found proteomic differences between Olfm4-H and Olfm4-L neutrophils in proteins relevant to neutrophil functions, we aimed to investigate potential functional differences. First, we used imaging flow cytometry to determine whether the subsets differ in their ability to respond to PMA with ROS production, as measured by oxidation of a fixable DNA-binding ROS dye (CellROX), followed by cell fixation and Olfm4 staining. Five minutes of PMA stimulation resulted in an increased CellROX

Fig. 2. Differential proteomic profiles of Olfm4-H and Olfm4-L neutrophil subsets in healthy blood donors. Olfm4-H and Olfm4-L neutrophils isolated from healthy blood donors ($n = 8$) were sorted by FACS and analysed by LC-MS/MS. **a** Volcano plot showing median log2 abundance ratios between the identified proteins in Olfm4-H and Olfm4-L neutrophils and their p values. **b** Left box-and-whisker plot showing proteins with a statistically significant positive median log2 abundance ratio, indicating increased abundance in the Olfm4-H neutrophils. Right box-and-whisker plot showing proteins with a statistically significant negative median log2 abundance ratio, indicating increased abundance in the Olfm4-L neutrophils. **c** Neutrophils from healthy blood donors ($n = 7$) were isolated and stained for proteins of interest and analysed by live imaging flow cytometry. Box-and-whisker plot comparing median fluorescence intensity of the immunofluorescently stained proteins Rab3d, S100A7, Rab3a, and CXCR1 between Olfm4-H and Olfm4-L neutrophils. Wilcoxon signed rank tests were used to test for statistical significance. Common contaminants and histones are not shown.

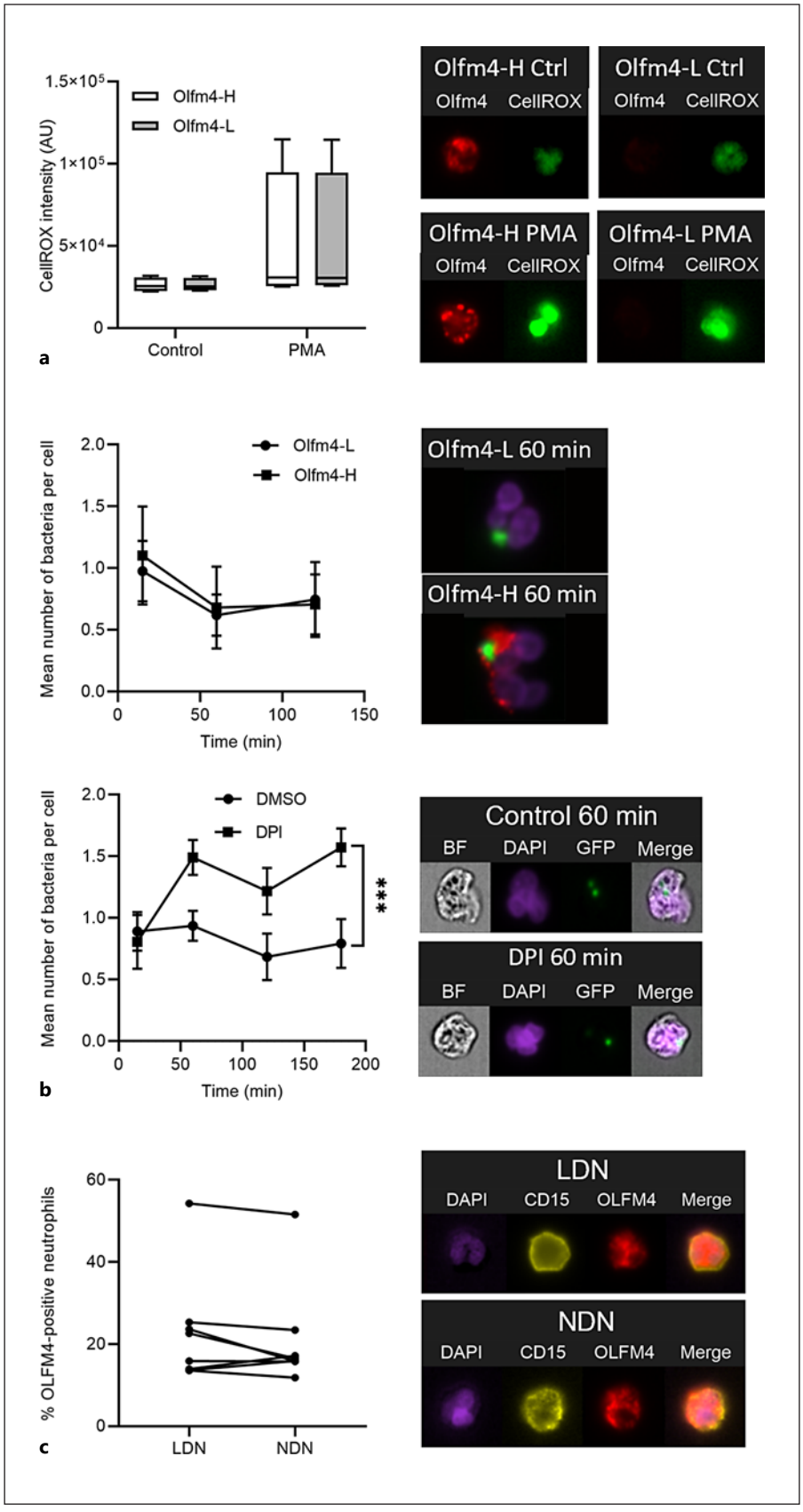

Fig. 3. In vitro functional comparison of Olfm4-H and Olfm4-L neutrophils. **a** For the ROS assay, neutrophils isolated from healthy donors (n = 4) were loaded with CellROX and stimulated with PMA or buffer for 5 min before fixation and Olfm4 staining. Diagram showing CellROX intensity in Olfm4-H and Olfm4-L subsets, as analysed by imaging flow cytometry. Statistical significance was tested by multiple Wilcoxon signed rank tests. Representative images are shown. **b** For the bacterial infection assay, *S. aureus* at MOI 10 was allowed to adhere on ice to neutrophils isolated from healthy donors (n = 6), followed by incubation at 37°C for the indicated times, fixation, Olfm4 staining, and analysis by imaging flow cytometry. Top diagram showing the mean (error bars show SD) number of bacteria per Olfm4-H or Olfm4-L neutrophil over time. Lower diagram showing the mean number of bacteria (error bars show 95% confidence intervals) per neutrophil over time in a control experiment (n > 150 neutrophils) where samples were treated with DPI or solvent control during infection. Statistical significance was tested by 2-way ANOVA. Representative images are shown. **c** The proportion of Olfm4-H neutrophils was analysed by imaging flow cytometry in LDNs (localizing to the PBMC layer during density gradient separation) and NDN (localizing to the granulocyte layer) of the same donors (n = 8), upon staining of cell surface CD15, to identify neutrophils, in combination with intracellular Olfm4. Diagram showing the percentage of Olfm4-H neutrophils in each neutrophil phenotype in each donor. Wilcoxon signed rank test was used to test for statistical significance. Representative images are shown.

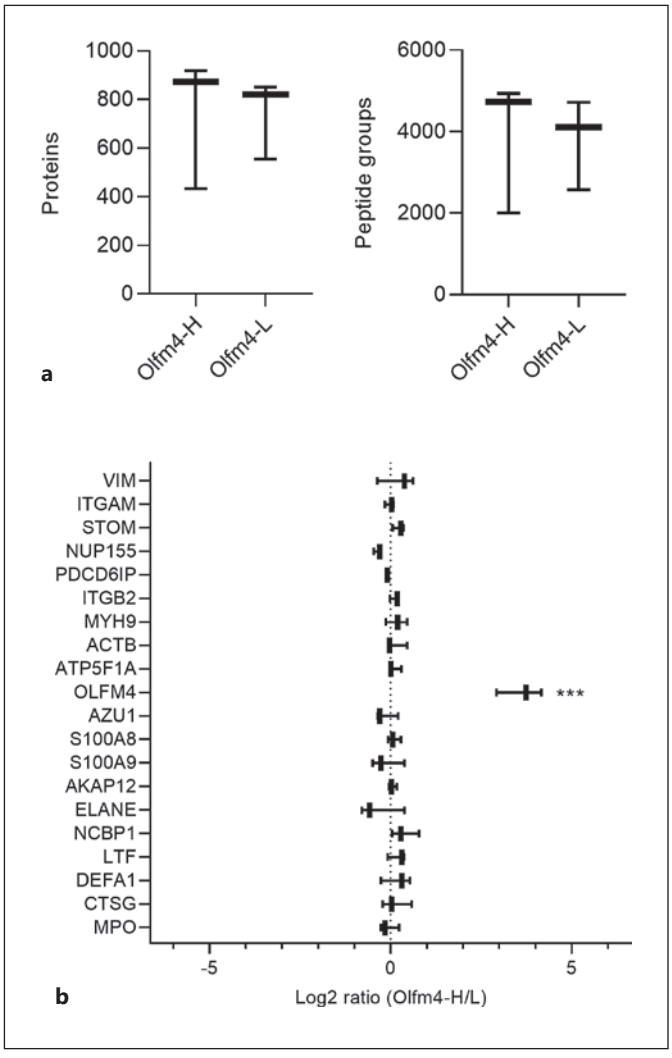

Fig. 4. Proteomic analysis of Olfm4-defined neutrophil subsets in patients with septic shock. Olfm4-H and Olfm4-L neutrophils isolated from patients with septic shock ($n = 3$) were sorted by FACS and analysed by LC-MS/MS. **a** Box-and-whisker plots showing the number of proteins and peptide groups identified in Olfm4-H and Olfm4-L neutrophil samples. **b** Box-and-whisker plot showing protein abundance log2 ratios for the 20 most abundant proteins between paired Olfm4-H/L neutrophil samples. Common contaminants and histones are not shown.

signal as compared to control, but no difference was observed between the Olfm4-defined subsets (Fig. 3a).

Several of the differently abundant proteins in the subsets are involved in the neutrophil response to infection and could potentially affect their ability to control bacteria. Thus, we developed an imaging flow cytometry-based assay quantifying the number of GFP-producing *S. aureus* inside or attached to neutrophils, after infection in suspension, fixation, and Olfm4 staining. However, there was no difference between Olfm4-H and Olfm4-L neutrophils regarding the number of bacteria per cell over time (Fig. 3b, top panel). The ability of the assay to detect differences in capacity to control *S. aureus* was confirmed by incubating the neutrophils with the NADPH-oxidase inhibitor diphenyleneiodonium chloride prior to infection, resulting in an increased number of bacteria over time ($p < 0.001$) as compared to the DMSO control (Fig. 3b, lower panel). Neutrophil killing of *S. aureus* is known to depend on the ability of the host cells to produce ROS through the NADPH-oxidase [20].

Due to their lower density, LDNs localize to the PBMC layer upon density gradient centrifugation. The LDNs are enriched in several inflammatory conditions and have been found to be increased in sepsis [21]. Recently, it has been proposed that the LDNs are part of the spectrum of the different densities found in healthy blood donors and which shifts during inflammation, owing e.g. to neutrophil activation, degranulation, or maturation [22]. Potential functional differences between Olfm4-H and Olfm4-L neutrophils could be related to neutrophil activation, and thus we compared Olfm4-H/L proportions in LDN and NDN. However, there was no difference in the percentage of Olfm4-H neutrophils between LDN and NDN from the same healthy blood donors (Fig. 3c).

The Olfm4-Defined Neutrophil Subsets Exhibit Proteomic Differences in Septic Shock

The data presented above disclosed that the Olfm4-defined subsets display different proteomic profiles at baseline, and the literature suggests a pathogenic role for Olfm4-H neutrophils in sepsis [4, 6, 23]. Accordingly, we hypothesized that the Olfm4-H neutrophils display a distinct proteomic profile also in septic shock.

The proteomes of FACS-sorted Olfm4-H and Olfm4-L neutrophils isolated from three patients with septic shock were analysed, using the same workflow as for healthy blood donors described above. A similar number of proteins and peptide groups were identified in both subsets (Fig. 4a). The total number of proteins found was 1,116, which was very similar to what was found for healthy blood donors. Online supplementary Table S3 lists all the identified proteins and their abundance in each subset in the patients. The most abundant proteins included S100A8/A9, azurocidin, neutrophil elastase, cathepsin G, lactoferrin, and myeloperoxidase (Fig. 4b). These proteins are comparable to the most abundant proteins in the healthy blood donor neutrophils, and none of the most abundant proteins apart from Olfm4 displayed

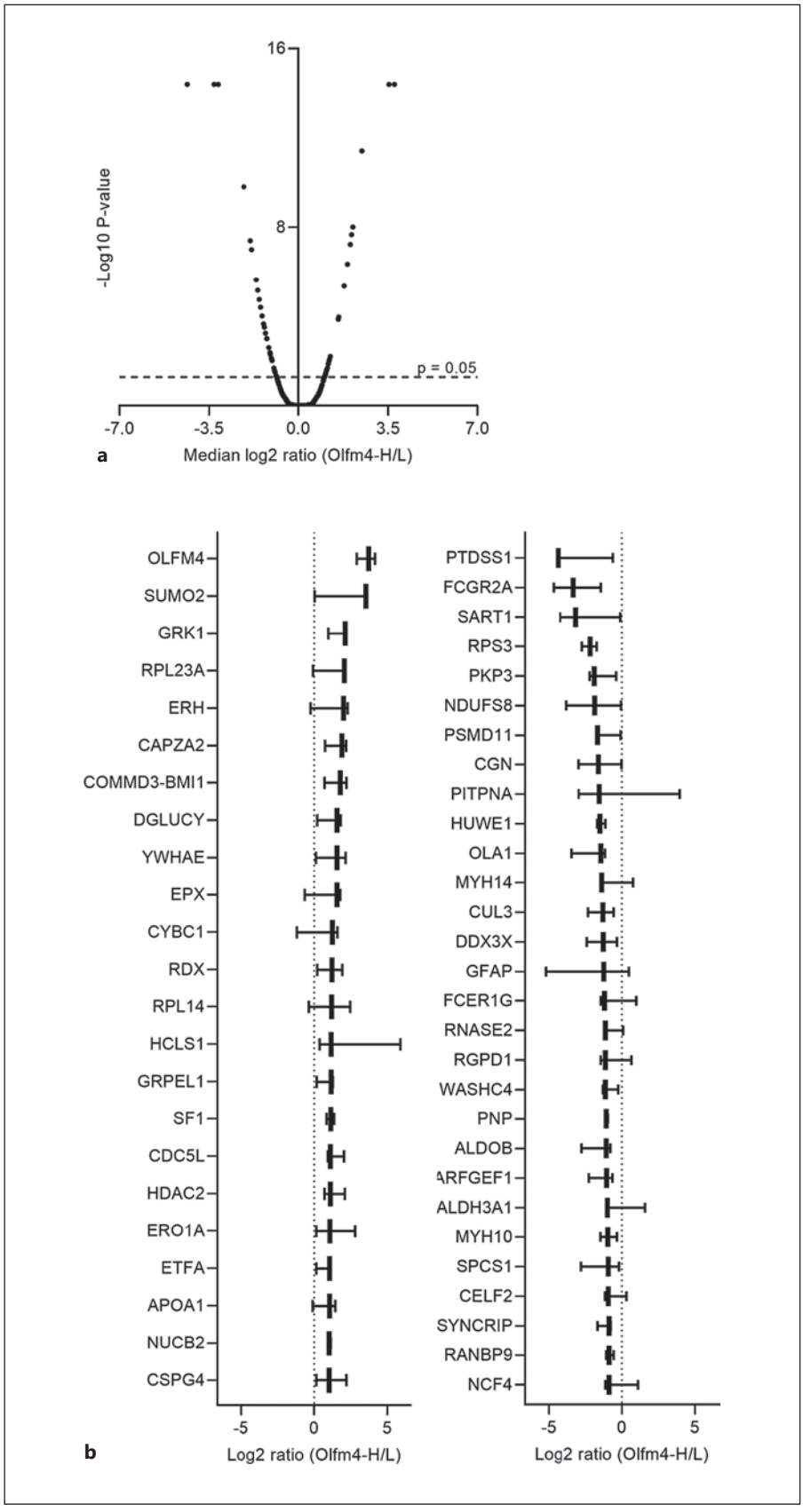

Fig. 5. Differential proteomic profiles of Olfm4-H and Olfm4-L neutrophil subsets in patients with septic shock. Olfm4-H and Olfm4-L neutrophils isolated from patients with septic shock (n = 3) were sorted by FACS and analysed by LC-MS/MS. **a** Volcano plot showing median log2 abundance ratios between the identified proteins in Olfm4-H and Olfm4-L neutrophils and their p values. **b** Left box-and-whisker plot showing proteins with a statistically significant positive median log2 abundance ratio, indicating increased abundance in the Olfm4-H neutrophils. Right box-and-whisker plot showing proteins with a statistically significant negative median log2 abundance ratio, indicating increased abundance in the Olfm4-L neutrophils. Common contaminants are not shown.

a significantly increased abundance in either of the subsets. Olfm4 was again among the 20 most abundant proteins in the Olfm4-H subset and had a median log2 ratio between the Olfm4-H and Olfm4-L subsets of 3.74, with a significance level of $p = 4 \times 10^{-15}$ (Fig. 4b).

A log2 abundance ratio between the Olfm4-H and Olfm4-L subsets with a p value of <0.05 was seen for 54 proteins, where 24 proteins were more abundant in the Olfm4-H and 30 in the Olfm4-L subset (Fig. 5a). Proteins such as cytochrome b-245 chaperone 1 displayed higher abundance in the Olfm4-H subset (Fig. 5b, left panel) and among others Fc gamma receptor 2a, Fc epsilon receptor 1 gamma subunit, Wiskott Aldrich Syndrome protein and scar homologue complex subunit 4, and neutrophil cytosolic factor 4 in the Olfm4-L subset (Fig. 5b, right panel). Thus, the profiles differed not only between the subsets but also between healthy controls and patients with septic shock. Pathway enrichment analysis showed no statistically significant enrichment in any pathway in either the Olfm4-H (online suppl. Table S4) or Olfm4-L (online suppl. Table S4) subset in the patients with septic shock.

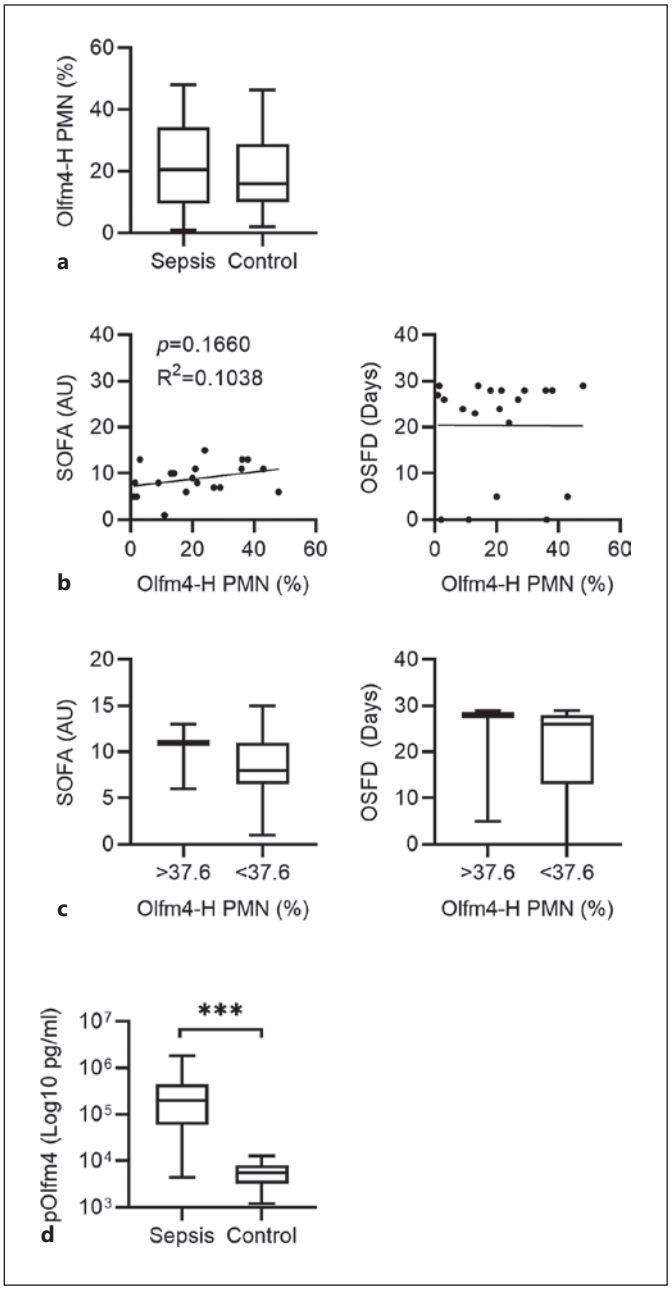

Olfm4-H Proportion and Plasma Olfm4 in Septic Shock

Having discovered proteomic differences between Olfm4-H and Olfm4-L neutrophils both at baseline and in septic shock, we finally sought to corroborate the correlation between the percentage of Olfm4-H neutrophils and disease severity [4, 6, 23] in an adult population of patients with septic shock admitted to the ICU at Linköping University Hospital. The Olfm4-proportions in whole blood neutrophils, as well as plasma Olfm4 concentrations, were analysed in 20 patients and 20 healthy blood donors. Data on SOFA score [11] on admission, where a higher score corresponds to a higher degree of organ dysfunction, and OSFD for the first 30 days [14], where a higher value means that the patient was alive and free of invasive organ support for a greater number of days during the first month, were collected. The mean admission SOFA score was 7.9 (median 8.5, range 1–15) and the mean OSFD was 20.4 (median 26, range 0–29).

Fig. 6. Analysis of Olfm4-H proportion and plasma Olfm4 concentration in patients with septic shock. Peripheral blood was collected from patients with septic shock ($n = 20$) and healthy blood donors ($n = 20$). The proportion of Olfm4-H neutrophils was analysed by imaging flow cytometry after fixation of leukocytes, staining of CD15 for neutrophil identification, permeabilization and antibody staining of Olfm4. **a** Box-and-whisker plot showing the proportion of Olfm4-H neutrophils in sepsis patients and healthy controls. **b** Scatterplots showing the correlation between the proportion of Olfm4-H neutrophils and SOFA score (left panel) or OSFD (right panel). **c** Box-and-whisker plots showing SOFA score (left panel) or OSFD (right panel) of sepsis patients with percentage of Olfm4-H neutrophils above 37.6% ($n = 3$) or below 37.6% ($n = 17$). **d** Olfm4 concentrations in plasma were quantified by ELISA. Box-and-whisker plots showing plasma Olfm4 concentrations in plasma obtained from patients with septic shock and healthy donors.

The proportion of Olfm4-H neutrophils was similar between patients with septic shock and healthy blood donors (Fig. 6a). The percentage of Olfm4-H neutrophils showed a non-significant correlation with SOFA score (Fig. 6b, left panel) and no tendency for correlation with OSFD (Fig. 6b, right panel). As the percentage of Olfm4-H neutrophils has previously been shown to predict mortality in septic shock, the patients were divided into those with a low versus high proportion of Olfm4-H neutrophils using the previously published cut-off of >37.6% [6]. Patients with a high proportion tended to have higher SOFA scores upon admission to the ICU, but the difference was not statistically significant (Fig. 6c, left panel) and there was no trend regarding OSFD (Fig. 6c, right panel). The concentration of plasma Olfm4 was drastically increased in patients with septic shock as compared to healthy controls (Fig. 6d). The Olfm4 plasma concentrations correlated with another neutrophil-specific granule protein, NGAL (online suppl. Fig. S5). Neutrophilia is a common finding in sepsis [24], and when the plasma Olfm4 values were normalized to the estimated number of neutrophils in the sample (based on the neutrophil concentration as recorded by imaging flow cytometry), there was no longer a significant difference between patients and controls (online suppl. Fig. S5). The plasma Olfm4 concentration showed no correlation with either SOFA score or OSFD (data not shown). In summary, the percentage of Olfm4-H neutrophils did not correlate significantly with the severity of septic shock. Meanwhile, patients with septic shock had drastically elevated concentrations of free Olfm4 in plasma, associated with neutrophilia.

Discussion and Conclusion

The proportion of Olfm4-H neutrophils has been found to correlate with the severity of septic shock [4, 6], but it is not known whether there are functional differences between the Olfm4-defined subsets in sepsis. Here, we establish that Olfm4 marks a neutrophil subset with a distinct proteomic profile in healthy individuals and patients with septic shock. However, the differences did not translate to apparent functional differences in vitro or in septic shock.

First, we deciphered the proteomic differences between the Olfm4-defined neutrophil subsets at baseline, using an adaptation of a published protocol [15]. This is to our knowledge the first report of the proteome of fixed, permeabilized, antibody-stained, and FACS-sorted neutrophils. In healthy blood donors, 1,136 proteins were identified by LC-MS/MS, similar to a previously published study of non-fixed human neutrophil granules identifying about 1,500 proteins [25]. Similar numbers of proteins were identified in both subsets, and major granule proteins were present in equal abundance in both subsets, as previously published for, e.g., NGAL [3] and gelatinase [2]. The only exception was the Olfm4 protein itself, which as expected was vastly more abundant in the Olfm4-H subset. The finding that the Olfm4 protein was detected in the Olfm4-L subset, albeit at a 24 times lower level than in the Olfm4-H, is in accordance with a previous study showing weak but specific immunoreactivity to anti-Olfm4 antibody in the Olfm4-L subset [2].

In healthy blood donors, both subsets showed enrichment in the neutrophil degranulation pathway. In the Olfm4-H cells, Rab3d, suggested to be involved in neutrophil degranulation [26], leucine-rich alpha-2 glycoprotein 1, secreted from peroxidase-negative neutrophil granules and regulating myelopoiesis [27], and the danger-associated molecular pattern high mobility group protein B1 showed higher abundance. Meanwhile, the chemotactic alarmin S100-A7 [28], Rab3a, suggested to be involved in neutrophil degranulation [29], CXCR1, a major neutrophil chemotactic receptor that binds interleukin-8 [30], and neutrophil defensin alpha 4, an antimicrobial peptide with bactericidal activity [31], showed higher abundance in the Olfm4-L neutrophils. Thus, the proteomic profiles of the subsets diverged, involving differences in proteins important for immunological and inflammatory processes in neutrophils. Collectively, the data may suggest different preparedness of the subsets to respond to microbial or inflammatory stimuli. Out of the significantly more abundant proteins in the Olfm4-H or Olfm4-L subset, only increased abundance of Rab3a in the Olfm4-L subset could be confirmed by immunofluorescent staining. We did not discover any protein other than Olfm4 with a bimodal distribution that can be used as a surrogate marker for Olfm4. At most, there was a subtle difference in overall protein level, and the differences in proteome likely reflect different dynamic profiles rather than fixed co-expressed proteins.

To translate the findings from proteomics into functional differences, we compared the ability of the Olfm4-H and Olfm4-L subsets to produce ROS in response to PMA and to control infection with *S. aureus*. The Olfm4-H/L proportions in LDN as compared to NDN were also analysed. However, there were no differences between the subsets in any of these respects. It is possible that the Olfm4 protein itself partakes in unfavour-

able processes, as an alternative to being a marker of a pathogenic subset. Employing knockout mice, it has previously been demonstrated that Olfm4 reduces the host ability to control bacterial infection [32, 33], that Olfm4 inhibits cathepsin C-mediated protease activities [33], and that Olfm4 increases hydrogen peroxide-induced apoptosis [34]. Olfm4-expressing mice display more severe mucosal damage in intestinal ischaemia-reperfusion injury [35] and juvenile Olfm4-decifient mice are protected from sepsis and acute kidney injury [23]. A recent study suggested a non-microbial mechanism being responsible for the ability of Olfm4-H proportion to predict death in critically ill patients [6]. All the mentioned studies support the idea of detrimental processes in Olfm4-H neutrophils, with defective bacterial clearance or an exaggerated pro-inflammatory response, a concept that was not clearly reflected in the presented data.

Extending our study to septic shock, we hypothesized that proteomic differences between the Olfm4-H and Olfm4-L subsets might contribute to sepsis pathogenesis. In patients with septic shock, as in healthy individuals, Olfm4 was the only major granule protein with a significantly increased abundance in one subset. The subsets again displayed distinct proteomic profiles, encompassing partly different proteins as compared to healthy donors, which could point to different functions of the individual subsets in health and in sepsis. However, due to the vastly different phenotypes of neutrophils in healthy individuals and patients with sepsis, with an increased presence of immature neutrophils in the latter [36], the profiles were not compared directly. Meanwhile, the proportion of Olfm4-H neutrophils itself does not appear to be affected by neutrophil maturation stage as the Olfm4 protein appears already in the bone marrow [2] and as there was no correlation between Olfm4-H proportion and band cell count in paediatric septic shock [4]. Interestingly, the cytochrome b-245 chaperone 1 protein, required for the optimal production of the main subunit ($gp91^{phox}$) of the neutrophil NAPDH oxidase and thus for the efficient production of ROS [37], was significantly increased in the Olfm4-H subset. The same protein displayed near-significant ($p = 0.099$) enrichment in the Olfm4-H subset in healthy individuals. Meanwhile, $gp91^{phox}$ itself (encoded by the *CYBB*, or *NOX2*, gene) was not more abundant in any subset. The cytosolic NADPH-oxidase subunit $gp40^{phox}$, also termed neutrophil cytosolic factor 4, was more abundant in the Olfm4-L cells, which also displayed increased abundance of Fc epsilon receptor 1 gamma subunit, involved in immunoreceptor signal transduction [38], the low-affinity IgG receptor Fc gamma receptor IIa, which activates neutrophils upon cross-linking [39], as well as WASH complex subunit 4, important for actin reorganization in endosomal trafficking [40].

Finally, we aimed to corroborate the correlation between the percentage of Olfm4-H neutrophils and disease severity in adults with septic shock [4, 6]. However, there was no significant correlation between severity of illness as measured by SOFA score or OSFD and proportion of Olfm4-H neutrophils, although there was such a trend regarding SOFA score. The median percentage of Olfm4-H neutrophils reported in patients with sepsis here was 20.5%, which is lower than the 25% reported previously in paediatric sepsis [4] and 26.6% in adult sepsis [6]. Using the published cut-off score of >37.6% for predicting mortality in adult sepsis [6] only 3 of the 20 patients herein qualified. The lack of correlation in the present data may be explained by the small sample size. On the other hand, our data confirmed the significantly higher plasma concentration of Olfm4 in patients with septic shock than in healthy controls, as reported for children [4]. The Olfm4 concentration was associated with neutrophil concentration and correlated with NGAL concentration, suggesting neutrophil origin.

In conclusion, the human Olfm4-defined neutrophil subsets display different proteomic profiles at baseline as well as in septic shock, pointing towards specific differential functions of the subpopulations. However, no such differences were found experimentally and there was no significant correlation between Olfm4-H proportion and severity of septic shock, pointing against a major contribution of the Olfm4-H subset to sepsis pathogenesis. Further studies are needed to delineate the biological and clinical significance of the discovered proteomic differences.

Preprint

A preprint version of this article is available on bioRxiv [41].

Acknowledgments

We are grateful to study nurses Helén Didriksson and Carina Jonsson for arranging the patient samples. Flow cytometry was performed using instruments at the Flow Cytometry Core Facility, Faculty of Medicine and Healthy Sciences, Linköping University. We would like to acknowledge the Proteomics Core Facility, Faculty of Medicine and Health Sciences, Linköping University, for assistance with proteomics and the Bioinformatics Core Facility,

Faculty of Medicine and Health Sciences and Clinical Genomics Linköping, SciLife Laboratory, Department of Biomedical and Clinical Sciences, Linköping University, for assistance with bioinformatic analyses.

Statement of Ethics

Peripheral blood from healthy blood donors was obtained through the Linköping University Hospital blood bank. The donors had given written consent that blood could be used for research purposes and only de-identified samples were received. In accordance with the Declaration of Helsinki and paragraph 4 of the Swedish law (2003:460) on Ethical Conduct in Human Research, no specific ethical approval is needed. Blood samples from patients with septic shock were obtained after approval of the study protocol by the regional ethical review board (Linköping 2016/361-31, 2018/631-32) and with informed written consent from the patient or next of kin.

Conflict of Interest Statement

The authors have no conflicts of interest to declare.

Funding Sources

The study was supported by grants from the Swedish Society of Medicine, the Åke Wiberg Foundation, the Medical Inflammation and Infection Center (MIIC), the Linköping Society of Medicine, and the Linköping University – Region Östergötland ALF agreement (935252, 969456).

Author Contributions

Amanda Welin conceived the study, planned the experiments, analysed the data, and wrote the manuscript together with Hans Lundquist and with input from all authors. In addition, Hans Lundquist performed experiments and analysed the data. Henrik Andersson and Michelle S. Chew provided access to patient samples and clinical data and contributed to the study design and data analysis. Jyotirmoy Das performed and contributed to interpretation of bioinformatic analysis. Maria V. Turkina contributed to development of the proteomics protocol, performed LC-MS/MS, and analysed proteomics data. All authors read and approved the final manuscript.

Data Availability Statement

All data generated or analysed during this study are included in this article and its online supplementary material files. Further enquiries can be directed to the corresponding author.

References

1 Deniset JF, Kubes P. Neutrophil heterogeneity: bona fide subsets or polarization states? J Leukoc Biol. 2018 May;103(5):829–38.
2 Clemmensen SN, Bohr CT, Rorvig S, Glenthoj A, Mora-Jensen H, Cramer EP, et al. Olfactomedin 4 defines a subset of human neutrophils. J Leukoc Biol. 2012 Mar;91(3):495–500.
3 Welin A, Amirbeagi F, Christenson K, Bjorkman L, Bjornsdottir H, Forsman H, et al. The human neutrophil subsets defined by the presence or absence of OLFM4 both transmigrate into tissue in vivo and give rise to distinct NETs in vitro. PLoS One. 2013;8(7):e69575.
4 Alder MN, Opoka AM, Lahni P, Hildeman DA, Wong HR. Olfactomedin-4 is a candidate marker for a pathogenic neutrophil subset in septic shock. Crit Care Med. 2017 Apr;45(4):e426–32.
5 Alder MN, Mallela J, Opoka AM, Lahni P, Hildeman DA, Wong HR. Olfactomedin 4 marks a subset of neutrophils in mice. Innate Immun. 2018 Dec 11;25(1):22–33.
6 Kangelaris KN, Clemens R, Fang X, Jauregui A, Liu T, Vessel K, et al. A neutrophil subset defined by intracellular Olfactomedin 4 is associated with mortality in sepsis. Am J Physiol Lung Cell Mol Physiol. 2021;320(5):L892–902.
7 Stark JE, Opoka AM, Fei L, Zang H, Davies SM, Wong HR, et al. Longitudinal characterization of olfactomedin-4 expressing neutrophils in pediatric patients undergoing bone marrow transplantation. PLoS One. 2020;15(5):e0233738.
8 Kassam AF, Levinsky NC, Mallela JP, Angel K, Opoka A, Lahni P, et al. Olfactomedin 4-positive neutrophils are upregulated after hemorrhagic shock. Am J Respir Cell Mol Biol. 2021 Feb;64(2):216–23.
9 Liu W, Rodgers GP. Olfactomedin 4 expression and functions in innate immunity, inflammation, and cancer. Cancer Metastasis Rev. 2016 Jun;35(2):201–12.
10 Rudd KE, Johnson SC, Agesa KM, Shackelford KA, Tsoi D, Kievlan DR, et al. Global, regional, and national sepsis incidence and mortality, 1990–2017: analysis for the Global Burden of Disease Study. Lancet. 2020 Jan 18;395(10219):200–11.
11 Singer M, Deutschman CS, Seymour CW, Shankar-Hari M, Annane D, Bauer M, et al. The third international consensus definitions for sepsis and septic shock (Sepsis-3). JAMA. 2016 Feb 23;315(8):801–10.
12 van der Poll T, van de Veerdonk FL, Scicluna BP, Netea MG. The immunopathology of sepsis and potential therapeutic targets. Nat Rev Immunol. 2017 Jul;17(7):407–20.
13 Wiersinga WJ, Leopold SJ, Cranendonk DR, van der Poll T. Host innate immune responses to sepsis. Virulence. 2014 Jan 1;5(1):36–44.
14 Bourcier S, Hindlet P, Guidet B, Dechartres A. Reporting of organ support outcomes in septic shock randomized controlled trials: a methodologic review: the sepsis organ support study. Crit Care Med. 2019 Jul;47(7):984–92.
15 Coscia F, Doll S, Bech JM, Schweizer L, Mund A, Lengyel E, et al. A streamlined mass spectrometry-based proteomics workflow for large-scale FFPE tissue analysis. J Pathol. 2020 May;251(1):100–12.
16 Cassatella MA, Ostberg NK, Tamassia N, Soehnlein O. Biological roles of neutrophil-derived granule proteins and cytokines. Trends Immunology. 2019 Jul;40(7):648–64.
17 Yu G, He Q-Y. ReactomePA: an R/Bioconductor package for reactome pathway analysis and visualization. Mol Biosyst. 2016;12(2):477–9.

18 Fabregat A, Korninger F, Viteri G, Sidiropoulos K, Marin-Garcia P, Ping P, et al. Reactome graph database: efficient access to complex pathway data. PLoS Comput Biol. 2018 Jan; 14(1):e1005968.
19 Schwartz J, Leidal KG, Femling JK, Weiss JP, Nauseef WM. Neutrophil bleaching of GFP-expressing staphylococci: probing the intraphagosomal fate of individual bacteria. J Immunol. 2009 Aug 15;183(4):2632–41.
20 Rada BK, Geiszt M, Kaldi K, Timar C, Ligeti E. Dual role of phagocytic NADPH oxidase in bacterial killing. Blood. 2004 Nov 1;104(9): 2947–53.
21 Sun R, Huang J, Yang Y, Liu L, Shao Y, Li L, et al. Dysfunction of low-density neutrophils in peripheral circulation in patients with sepsis. Sci Rep. 2022 Jan 13;12(1):685.
22 Hassani M, Hellebrekers P, Chen N, Aalst C, Bongers S, Hietbrink F, et al. On the origin of low-density neutrophils. J Leukoc Biol. 2020 May;107(5):809–18.
23 Stark JE, Opoka AM, Mallela J, Devarajan P, Ma Q, Levinsky NC, et al. Juvenile OLFM4-null mice are protected from sepsis. Am J Physiology Renal Physiol. 2020 Mar 1;318(3): F809–16.
24 Shen XF, Cao K, Jiang JP, Guan WX, Du JF. Neutrophil dysregulation during sepsis: an overview and update. J Cell Mol Med. 2017 Sep;21(9):1687–97.
25 Rorvig S, Ostergaard O, Heegaard NHH, Borregaard N. Proteome profiling of human neutrophil granule subsets, secretory vesicles, and cell membrane: correlation with transcriptome profiling of neutrophil precursors. J Leukoc Biol. 2013 Oct;94(4):711–21.
26 Prashar A, Schnettger L, Bernard EM, Gutierrez MG. Rab GTPases in immunity and inflammation. Front Cell Infect Microbiol. 2017;7:435.
27 Druhan LJ, Lance A, Li S, Price AE, Emerson JT, Baxter SA, et al. Leucine rich alpha-2 glycoprotein: a novel neutrophil granule protein and modulator of myelopoiesis. PLoS One. 2017;12(1):e0170261.
28 Wolf R, Howard OMZ, Dong HF, Voscopoulos C, Boeshans K, Winston J, et al. Chemotactic activity of S100A7 (Psoriasin) is mediated by the receptor for advanced glycation end products and potentiates inflammation with highly homologous but functionally distinct S100A15. J Immunol. 2008 Jul 15;181(2): 1499–506.
29 Ramadass M, Catz SD. Molecular mechanisms regulating secretory organelles and endosomes in neutrophils and their implications for inflammation. Immunol Rev. 2016 Sep;273(1):249–65.
30 Metzemaekers M, Gouwy M, Proost P. Neutrophil chemoattractant receptors in health and disease: double-edged swords. Cell Mol Immunol. 2020 May;17(5):433–50.
31 Lehrer RI, Lu W. α-Defensins in human innate immunity. Immunological Rev. 2012 Jan;245(1):84–12.
32 Liu W, Yan M, Liu Y, Wang R, Li C, Deng C, et al. Olfactomedin 4 down-regulates innate immunity against *Helicobacter pylori* infection. Proc Natl Acad Sci U S A. 2010 Jun 15; 107(24):11056–61.
33 Liu W, Yan M, Liu Y, McLeish KR, Coleman WG Jr, Rodgers GP. Olfactomedin 4 inhibits cathepsin C-mediated protease activities, thereby modulating neutrophil killing of *Staphylococcus aureus* and *Escherichia coli* in mice. J Immunol. 2012 Sep 1;189(5):2460–7.
34 Liu W, Liu Y, Li H, Rodgers GP. Olfactomedin 4 contributes to hydrogen peroxide-induced NADPH oxidase activation and apoptosis in mouse neutrophils. Am J Physiol Cell Physiol. 2018 Oct 1;315(4):C494–501.
35 Levinsky NC, Mallela J, Opoka AM, Harmon K, Lewis HV, Zingarelli B, et al. The olfactomedin-4 positive neutrophil has a role in murine intestinal ischemia/reperfusion injury. FASEB J. 2019 Dec;33(12):13660–8.
36 Shen X, Cao K, Zhao Y, Du J. Targeting neutrophils in sepsis: from mechanism to translation. Front Pharmacol. 2021;12:644270.
37 Arnadottir GA, Norddahl GL, Gudmundsdottir S, Agustsdottir AB, Sigurdsson S, Jensson BO, et al. A homozygous loss-of-function mutation leading to CYBC1 deficiency causes chronic granulomatous disease. Nat Commun. 2018 Oct 25;9(1):4447.
38 Nemeth T, Futosi K, Szabo M, Aradi P, Saito T, Mocsai A, et al. Importance of Fc receptor gamma-chain ITAM tyrosines in neutrophil activation and in vivo autoimmune arthritis. Front Immunol. 2019;10:252.
39 Wang Y, Jonsson F. Expression, role, and regulation of neutrophil Fcγ receptors. Front Immunol. 2019;10:1958.
40 Helfer E, Harbour ME, Henriot V, Lakisic G, Sousa-Blin C, Volceanov L, et al. Endosomal recruitment of the WASH complex: active sequences and mutations impairing interaction with the retromer. Biol Cell. 2013 May;105(5): 191–207.
41 Lundquist H, Andersson H, Chew MS, Das J, Turkina MV, Welin A. The Olfm4-defined human neutrophil subsets differ in proteomic profile in septic shock. bioRxiv. 2022 Mar 9. Epub ahead of print.